ISBN: 978-3-95450-230-1 ISSN: 2673-5350 doi:10.18429/JACoW-IBIC2021-WEPP28

SUB-ns SINGLE-PARTICLE SPILL CHARACTERIZATION FOR SLOW EXTRACTION

T. Milosic*, R. Singh, P. Forck
GSI Helmholtz Centre for Heavy Ion Research, Darmstadt, Germany

Abstract

With the recent developments on improving spill quality at GSI/FAIR, appropriate measurement devices have come into focus again. In contrast to commonly used scaler-based approaches where events at a certain sample frequency are counted, we present a measurement concept resolving single-event detector timestamps in the sub-ns regime leveraging a well-established off-the-shelf TDC VMEbus module. This allows for high-resolution time structure information with respect to the ring RF as well as evaluation of inter-particle separation distributions. This yields insightful information for specific experiments at GSI whose efficiencies are heavily limited by pile-ups and detector dead times. We will present the concept of the measurement setup and exemplary data taken in recent campaigns in context of spill microstructure improvements for slow extraction.

INTRODUCTION

Recent experiments measuring and optimizing slow-extraction spills at GSI/FAIR led to promising results [1]. The focus on spill quality introduced the demand to complement traditional counter-based approaches with single-particle detection at higher time resolution. Ideally, this would allow to resolve bunches and directly access the particle-interval information. Both is not possible with scalers even at high latching rates.

This goal can be achieved by fast time-to-digital converters (TDCs). They turn logic input signals, such as discriminated detector signals, into precise timestamps. Figure 1 schematically depicts timing events derived from two input signals and recorded by a TDC. Time-structure information

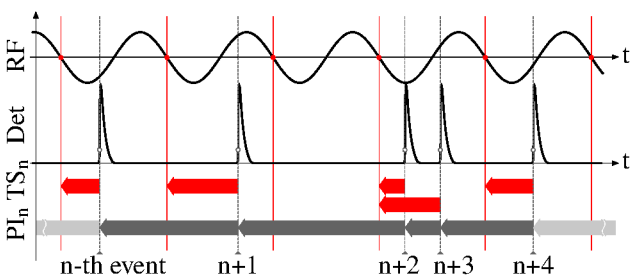


Figure 1: Single-particle events used to characterize spills.

is extracted from the detector event by correlating it with the SIS18 cavity RF or, alternatively, with a custom clock. The red arrows TS_n mark the difference between a detector event and the preceding slope-sensitive zero-crossing of the RF reference. This data is histogrammed at a user-definable bin size and time slice, providing a reconstruction of the time structure confined to the RF period range.

Similarly, the particle-interval (also *separation*) information PI_n is retrieved as the difference between consecutive detector timestamps as represented by gray arrows. Event data grouped in time slices is histogrammed with user-definable bin sizes and total range. The particle-interval distribution is useful to evaluate and optimize reduced efficiencies as a consequence of dead times of specific experiments.

Two application targets are considered. An online tool allows to asses spill characterization for operating and experiments. Furthermore, offline analysis preserving full information of the raw data is available. The TDC module comes with some limitations for which, in particular high-performance, online analysis is a challenge. However, the setup presented is capable to make use of the TDC ASICs performance to its fullest even in online mode.

HARDWARE SETUP

A system leveraging a high-precision TDC already existed as part of the ABLAX suite [2]. It is based on a RIO3 VMEbus controller, a CAEN V1290N TDC module and a custom software stack on top of LynxOS. Being limited to a net detection rate of $\ll$ 100 kEvents/s and the increasing challenge to maintain the environment this gave rise to a new development from scratch but using the same TDC module.

Constrained to the VMEbus, the new system uses a x86-64 MEN A25 controller [3] paired with a PMC White Rabbit FAIR timing receiver node (FTRN) [4] (Fig. 2). The con-

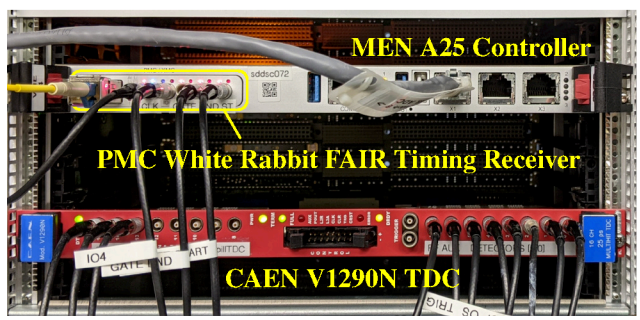


Figure 2: VMEbus mainframe configuration.

troller is based on the Intel(R) Pentium(R) CPU D1519 with 4 cores supporting 2 threads per core through hyper-threading at 1.50 to 2.10 GHz and 8 GiB of RAM. It has been equipped with a 1 TB mSATA SSD to store data locally.

Time-to-Digital Converter

The V1290N TDC VMEbus module is build around CERN's HPTDC ASIC [5] and is still available from CAEN.

* t.milosic@gsi.de

Content from this work may be used under the terms of the CC BY 3.0 licence (© 2021). Any distribution of this work must maintain attribution to the author(s), title of the work, publisher, and DOI

ISBN: 978-3-95450-230-1 ISSN: 2673-5350 doi:10.18429/JACoW-IBIC2021-WEPP28

Featuring two HPTDC ASICs, each serving 8 NIM inputs, 16 channels are available in total. A single ASIC is expected to be able to process a total maximum event rate of 4 MEvents/s at a double-hit resolution of 5 ns. Events are recorded with a native 21-bit timestamp counter. The TDC is operated in *Continuous Storage Mode* interleaving all recorded events in a sequential data stream. An RMS time resolution of 35 ps per input channel is achieved.

IMPLEMENTATION

The software stack implements a C++ FESA [6] class and a JavaFX GUI application. Additionally, an exporter is available to convert recorded binary data for offline data analysis. In the following, an overview on the most important aspects of the FESA class implementation is given.

Having an online mode for the DAQ was an essential requirement for operating and experiments. This complements the option to dump stream data containing full event information for in-depth offline analysis. However, online processing of data while being able to exploit the full event rate of the HPTDCs is challenging. The V1290N TDC module comes with some limitations that need to be considered carefully. With a 32-bit data word only 21 bits represent the timestamp to additionally accommodate headers and state flags. The counter value is mapped to time by a calibration factor, also called *least significant bit* (LSB) in this context. By applying a precise regular clock and a subsequent linear fit this yields a calibrated LSB time value of 24.414 ps. Consequently, the resulting dynamic range is only $2^{21} \cdot 24.414\,\text{ps} = 51.2\,\mu\text{s}$. Hence, manual overflow correction is mandatory with spill lengths up to several tens of seconds. At the same time, strict chronological order of TDC events is not guaranteed in the sequential stream of data. Unfortunately, this rules out the trivial approach to overflow correction by checking if $t_{n+1} < t_n$ for any consecutive recorded events. Just following that rule, without correcting ordering mismatches first, would lead to severe inconsistencies. This, among other compute-intensive tasks like prefetching the rate-divided RF timestamps, suggests to parallelize the data processing in order to leverage full performance of the HPTDC ASICs and avoid stalling of the acquisition and processing pipeline.

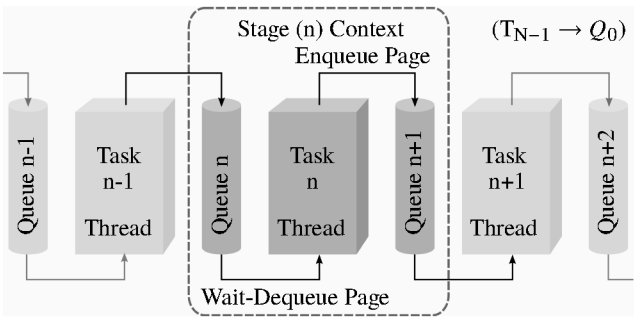


Figure 3: Pipeline concept with chained stages. Closed cycle: Last task N-1 outputs to queue 0 again.

Pipeline

The processing cycle is divided into sequential tasks representing separate stages of a pipeline. This is depicted schematically in Fig. 3. Each stage context consists of at least one input and one output queue (FIFO) accompanied by a thread processing a dedicated task along the pipeline. The thread dequeues a pointer to a page from the input queue, processes it and enqueues it to the output queue. A page, in this context, is defined as the data read from the TDC output buffer per acquisition cycle. By allocating a block of memory on the heap once and segment it into contiguous pages no further dynamic allocation will be required which avoids object creation and copy overhead. Flow control within the pipeline is provided by means of queues holding pointers to pages. At program initialization all pages are enqueued into the first queue of the pipeline maintaining their order. Moreover, synchronization is implicitly provided by the queue concept running as single-consumer single-producer at all stages. The pipeline is running in a closed cycle with the last stage outputting/enqueueing to the first queue again.

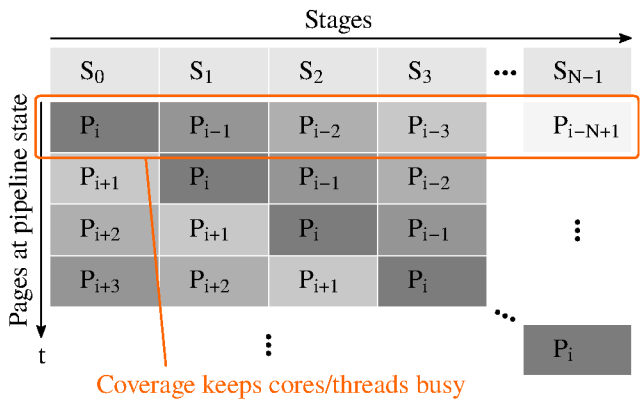


Figure 4: Coverage diagram for a pipeline with N stages.

Thread coverage is shown in Fig. 4. As processing progresses pages are transferred through the pipeline. Each stage is busy with a dedicated task but operates on a different page. This targets modern multi-core systems to distribute workloads.

The implementation features two coupled pipelines operating on pages of different word sizes. This is necessary to account for a larger dynamic range after manual overflow correction. With the longer word size of the second pipeline, 48 bits are used for the extended counter holding overflow-corrected timestamp values instead of the native 21 bits of the TDC. Thereby, the dynamic range is increased from 51.2 µs to more than 114 minutes while accuracy and precision is still preserved at the original LSB of 24.414 ps.

Figure 5 lists the stages, eight in total, for the two pipelines. Data flow starts at a tight acquisition loop on the TDC, reading data once a fill threshold of the output FIFO is met. The further stages will restore the chronological ordering and prefetch RF events. Overflow correction is the last stage of the first pipeline and provides coupling. It is also the first stage of the second pipeline at the same time and, thus, the

Content from this work may be used under the terms of the CC BY 3.0 licence (© 2021). Any distribution of this work must maintain attribution to the author(s), title of the work, publisher, and DOI

ISBN: 978-3-95450-230-1 ISSN: 2673-5350 doi:10.18429/JACoW-IBIC2021-WEPP28

Content from this work may be used under the terms of the CC BY 3.0 licence (© 2021). Any distribution of this work must maintain attribution to the author(s), title of the work, publisher, and DOI

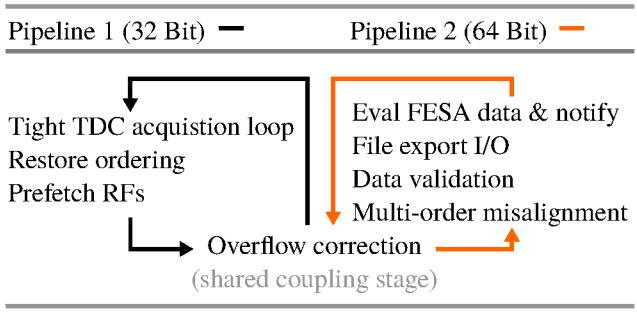


Figure 5: Data flow and tasks.

only stage reading and writing from two queues. Data flow in the second pipeline continues by checking for multi-order misalignments (occurs rarely at high rates) followed by a validation stage for data consistency. After passing the I/O stage, FESA data is prepared and properties are notified.

USER INTERFACE

A Java application, which is the typical interface for FESA classes at GSI, allows to view TDC data online. Common users are operators, experts from beam instrumentation and accelerator physics. The GUI application is depicted in Fig. 6. Configuration items are related to detector selectors,

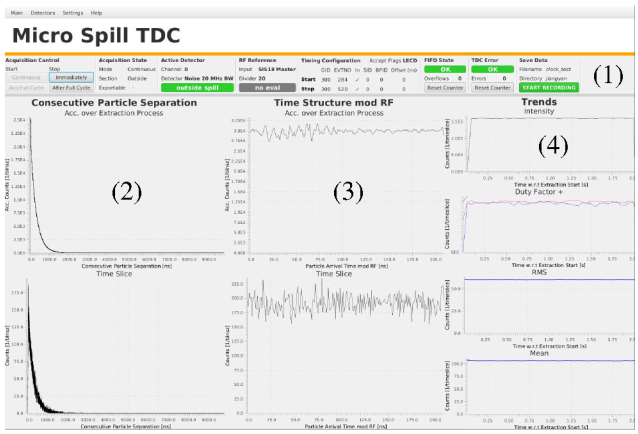


Figure 6: Remote Java GUI interfacing the FESA class.

timing configuration and RF reference (SIS18 native or AUX clock). Furthermore, bin sizes, ranges and global time slice duration can be configured but have no effect on stored data. Dumped data is based on single-event timestamps and, thus, preserves full detector information acquired in the first place. Time slices define the size of the time window within which data is evaluated.

The top row (1) features some configuration items, but also information about the current detector rate and acquisition status (output FIFO overflows and TDC errors).

Users can track particle-interval distributions in the left column (2). Time-structure information is presented to the user in the middle column (3). In both cases, the bottom row shows data of a single time slice. The top row is the accumulated information w.r.t. the current spill. For the screenshot a noise generator was attached providing a Poisson-like particle-interval distribution (left column). At the same time, events are not correlated with the RF, thus, the time structure is flat (middle column).

The right column (4) features a time series of parameters evaluated for each time slice along the spill. From top to bottom: intensity (current), duty factor [7] as well as mean and RMS of the time structure.

MEASUREMENTS

In the following, typical data analysis will be presented using the aforementioned exporter. Three targets are supported: time structures, particle-interval distributions and a high-res intensity/current mode. In all cases it is possible to superimpose spills with the high precision of the White-Rabbit timing [4] and, thus, enhance statistics. This is accomplished by injecting the spill start and end timing events into the data stream as TDC inputs generated by the FTRN. Beyond file information, the exporter supports filtering and selections of spills. This is handy in case of accidental timing settings recording different spills shared on the beam line. Filtering works on the basis of counts per spill and spill length. Additionally, the exporter supports selecting spills by range or index cherry-picking.

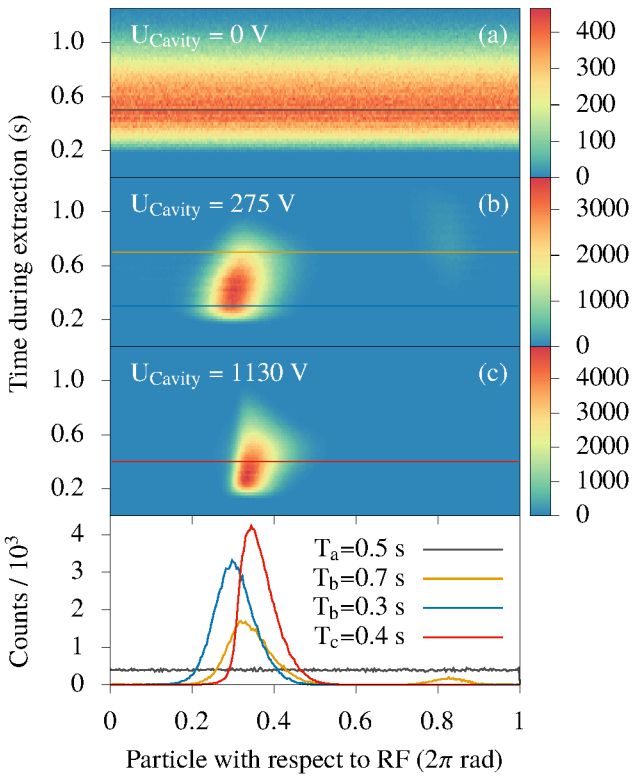


Figure 7: Time-structure information for Bi^{68+} beam.

Time Structure

A Bi^{68+} beam at 300 MeV/u recorded with a plastic scintillator is plotted in Fig. 7. Data is shown within a full RF period on the x axis and the time during extraction w.r.t. spill

ISBN: 978-3-95450-230-1 ISSN: 2673-5350 doi:10.18429/JACoW-IBIC2021-WEPP28

start on the y axis. Each row represents a time slice exported with 20 ms. The top data at a cavity voltage of 0 V clearly hints an unbunched beam with no correlation w.r.t. the RF. The time slice at $T_a = 0.5$ s confirms this with a flat time structure. At a cavity voltage of 275 V the beam is bunched but a second bunch emerges during extraction as can be seen in the bottom window for time slices at $T_b = 0.3$ s and 0.7 s. With a cavity voltage of 1130 V only one bunch is present but position and shape varies during extraction. Further interpretation of data is outside the scope of this paper.

Particle Intervals

Based on the same recorded data used for the time-structure before, Fig. 8 depicts particle-interval information for three different cavity voltages. The bottom window

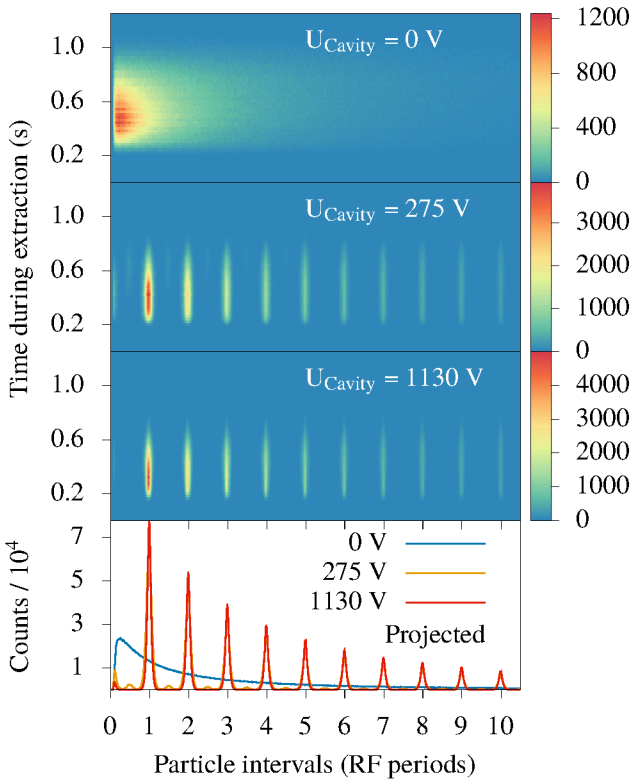


Figure 8: Particle-interval distribution for Bi^{68+} beam.

shows the projection onto the x axis given in units of RF periods. For 0 V cavity amplitude, the particle arrival interval is governed by a Poisson process. The resulting exponential interval distribution is apparent from the projection. At a cavity voltage of 275 V a pattern is visible with distinct accumulation regions evenly spaced by the RF. The projection reveals a second accumulation in between the prominent regions. At 1130 V only the prominent regions remain.

Spill Characterization

The slow extraction spill characterization using scaler data is discussed in [7]. Although the duty factor and maximum-to-mean ratio give a measure of the smoothness of the spill, it is not a direct quantification of the potential events and triggers seen by the experimental detectors. The time of arrival measured at the TDC provides a more direct measure of the usable part of a spill for a given detector response. Figure 9 shows a cumulative density function (CDF) of the

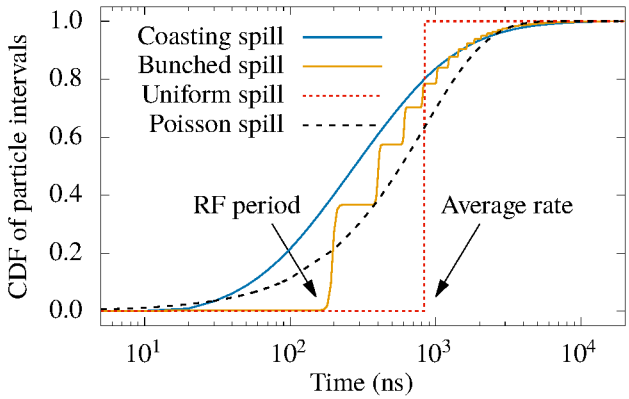


Figure 9: Cumulative distribution of the spills.

particle intervals for a coasting slow extraction spill and bunched beam spill along with the hypothetical Poisson and uniform spills at the same extraction rate. The rate for the spills shown was $1.2 \cdot 10^6$/s and extraction duration was 10 s. The jumps in the bunched beam extraction correspond to the 205 ns and its multiples i.e. RF period, which represents the temporal separation between particles maintained by the RF cavities. Bunched beam is known to mitigate the spill modulation caused by low frequency power supply ripples due to synchrotron motion at the cost of introducing high frequency structures at RF frequency [8]. It is evident, that there is a higher proportion of particles with larger time intervals for the bunched beam in comparison to coasting beam extraction. For some detector dead times, the correlations at RF periods can even be advantageous. An example of such a case is visible in Fig. 9; if a hypothetical detector has a dead time of 250 ns after arrival of every particle or event, bunched beam extraction provides potentially larger event rates in comparison to purely random Poisson statistics for the given extraction rate. Thus, the extraction rate and RF period has to be carefully chosen to benefit from bunched beam extraction.

SUMMARY

We presented a newly developed measurement setup for spill characterization based on an off-the-shelf TDC. Its implementation concept to leverage full TDC performance even in online mode was outlined. Experimental data highlights the additional and relevant information beyond what scalers can provide. The setup is used in regular operations providing a GUI application targeting different user groups. A feature-rich exporter is available to transform stored data streams for in-depth data analysis.

ACKNOWLEDGEMENT

We thank P. Boutachkov for helpful discussions on experimental detector dead times.

Content from this work may be used under the terms of the CC BY 3.0 licence (© 2021). Any distribution of this work must maintain attribution to the author(s), title of the work, publisher, and DOI

ISBN: 978-3-95450-230-1 ISSN: 2673-5350 doi:10.18429/JACoW-IBIC2021-WEPP28

Content from this work may be used under the terms of the CC BY 3.0 licence (© 2021). Any distribution of this work must maintain attribution to the author(s), title of the work, publisher, and DOI

REFERENCES

[1] R. Singh, P. Forck, and S. Sorge, "Reducing fluctuations in slow-extraction beam spill using transit-time-dependent tune modulation," *Phys. Rev. Applied*, vol. 13, p. 044 076, 4 Apr. 2020. DOI: 10.1103/PhysRevApplied.13.044076. https://link.aps.org/doi/10.1103/PhysRevApplied.13.044076

[2] T. Hoffmann, P. Forck, and D. A. Liakin, "New spill structure analysis tools for the vme based data acquisition system ablass at gsi," *AIP Conference Proceedings*, vol. 868, no. 1, pp. 343–350, 2006. DOI: 10.1063/1.2401422. https://aip.scitation.org/doi/abs/10.1063/1.2401422

[3] A. Wujek, D. Cobas, G. Daniluk, and M. Suminski. "Status and plans for the men-a25 vme cpu." BI/TB on uTCA, LIU wire-scanner results and AWAKE status. (Sep. 2017), https://indico.cern.ch/event/659372/contributions/2703686/attachments/1523293/2380688/A25_BI-TB.pdf

[4] C. Prados *et al.*, "Fair timing system developments based on white rabbit," in *Proc. 14th Int. Conf. on Accelerator and Large Experimental Physics Control Systems (ICALEPCS'13)*, (San Francisco, CA, USA), Oct. 2013, pp. 1288–1291. https://accelconf.web.cern.ch/ICALEPCS2013/papers/thppc092.pdf

[5] J. Christiansen, "Hptdc high performance time to digital converter," CERN, Geneva, Tech. Rep., 2004, Version 2.2 for HPTDC version 1.3. https://cds.cern.ch/record/1067476

[6] M. Arruat *et al.*, "Front-end software architecture," in *Proc. 11th Int. Conf. on Accelerator and Large Experimental Physics Control Systems (ICALEPCS'07)*, Knoxville, TN, USA, 2007, p. 310. http://cds.cern.ch/record/1093646

[7] R. Singh, P. Boutachkov, P. Forck, S. Sorge, and H. Welker, "Slow Extraction Spill Characterization From Micro to Milli-Second Scale," in *Proc. 9th International Particle Accelerator Conference (IPAC'18), Vancouver, BC, Canada, April 29-May 4, 2018*, (Vancouver, BC, Canada), ser. International Particle Accelerator Conference, https://doi.org/10.18429/JACoW-IPAC2018-WEPAK007, Geneva, Switzerland: JACoW Publishing, Jun. 2018, pp. 2095–2098, ISBN: 978-3-95450-184-7. DOI: doi:10.18429/JACoW-IPAC2018-WEPAK007. http://jacow.org/ipac2018/papers/wepak007.pdf

[8] S. Sorge, P. Forck, and R. Singh, "Measurements and Simulations of the Spill Quality of Slowly Extracted Beams from the SIS-18 Synchrotron," in *Proc. 9th International Particle Accelerator Conference (IPAC'18), Vancouver, BC, Canada, April 29-May 4, 2018*, (Vancouver, BC, Canada), ser. International Particle Accelerator Conference, https://doi.org/10.18429/JACoW-IPAC2018-TUPAF081, Geneva, Switzerland: JACoW Publishing, Jun. 2018, pp. 924–926, ISBN: 978-3-95450-184-7. DOI: doi:10.18429/JACoW-IPAC2018-TUPAF081. http://jacow.org/ipac2018/papers/tupaf081.pdf